Environ Earth Sci (2015) 74:2531–2538
DOI 10.1007/s12665-015-4271-4

ORIGINAL ARTICLE

Detrended fluctuation analysis of spatial patterns on urban impervious surface

Qin Nie[1] · Jianhua Xu[2] · Wang Man[1] · Fengqin Sun[1]

Received: 21 August 2014 / Accepted: 3 March 2015 / Published online: 10 March 2015
© Springer-Verlag Berlin Heidelberg 2015

Abstract This paper analyzes satellite data from downtown Shanghai, China, to investigate the long-range dependence of spatial patterns on urban impervious surfaces (UIS) using two-dimensional detrended fluctuation analysis (DFA). The UIS fraction is estimated from Landsat Thematic Mapper and Enhanced Thematic Mapper Plus data from 1997 to 2010 using linear spectral mixture analysis. The results indicate that the spatial distribution of the UIS exhibits a positive spatial dependence, as revealed by Moran's index, capturing the evolution from aggregation to dispersion and back to aggregation during the study period. The use of two-dimensional DFA reveals a strong long-range power-law dependence in the UIS spatial pattern during the study period. The DFA scaling exponent can be seen as a measure of the uniformity of the UIS spatial distribution, and exhibits an approximate $1/f$ behaviour. Two-dimensional multifractal detrended fluctuation analysis (MFDFA) confirmed that the UIS spatial pattern is not multifractal in nature, meaning that only a single scaling exponent is required to disclose the long-range dependence in the UIS spatial pattern. The application of two-dimensional DFA to UIS patterns should be viewed as a complementary tool to existing techniques, such as Fourier analysis, wavelets, and structure function, that can provide additional information about the structure of UIS patterns, including its $1/f$ behaviour.

✉ Qin Nie
nieqinhongyi@163.com

[1] Department of Spatial Information Science and Engineering, Xiamen University of Technology, Xiamen 361024, China

[2] The Research Center for East-West Cooperation in China, The Key Lab of GIScience of the Education Ministry PRC, East China Normal University, Shanghai 200241, China

Keywords Urban impervious surface · Spatial pattern · Two-dimensional detrended fluctuation analysis

Introduction

Urbanisation and urban sprawl have become major concerns in China since the nineteenth century. Changes in land cover types from permeable land to anthropogenic impervious surfaces have occurred alongside population growth. The urban impervious surface (UIS) fraction is a key metric for identifying the spatial extent and intensity of urbanisation and urban sprawl (Clapham 2003), as well as assessing urban environments. Understanding the UIS spatial pattern has thus become a pervasive scientific topic in urban settings.

Numerous studies have been conducted to reveal local UIS patterns, where the description and comparison of the UIS spatial pattern are primarily used to characterise the evolution of the urban environment (Bauer et al. 2004; Dougherty et al. 2004; Rashed 2008; Relly et al. 2004; Xian and Crane 2006). Although recent research has shown that UIS spatial pattern exhibits a strong spatial dependence (Liu et al. 2011; Xie et al. 2009), as indicated through spatial autocorrelation analysis, these trends in UIS spatial pattern require further investigation. These studies, which generally employ a single spatial autocorrelation coefficient, reveal the spatial dependence of UIS pattern from only a single spatial scale. To accurately map the spatial pattern from different spatial scales, it is thus necessary to calculate multiple autocorrelation coefficients across different spatial scales.

It has been recently realised that fractal geometry can be applied to measure the spatial complexity of UIS pattern, where the magnitude of the fractal dimension identifies the

degree of complexity of the UIS spatial pattern. Existing fractal studies of UIS pattern can be summarised as either one-dimensional fractal along section lines (Liu et al. 2011) or morphological fractal of UIS patches (Liu et al. 2012; Xie et al. 2009). Deeper fractal properties, such as the long-range dependence of the UIS spatial pattern, have been rarely studied, and no substantial research has attempted to detect the two-dimensional long-range dependence of the UIS spatial pattern.

Detrended fluctuation analysis (DFA) is a modified root-mean-square nonlinear dynamic random walk analysis. The advantage of DFA over conventional methods, such as R/S and spectral analyses, is that it cannot only preserve the persistence or anti-persistence of the original series, but also removes the obvious self-similarity resulting from the possible trends. DFA employs only a single scaling exponent to characterise the long-range dependence in the series, whereas multifractal detrended fluctuation analysis (MFDFA), using a set of scaling exponents, can analyse the long-range dependence from multiple levels. Gu and Zhou (2006) successfully generalised the one-dimensional DFA and MFDFA to a two-dimensional framework. Consequently, two-dimensional DFA and MFDFA have been widely used in various studies, yielding correct results for a two-dimensional array and more in-depth information (Gu and Zhou 2006; Raoufi et al. 2008; Moktadir et al. 2008; Barrera et al. 2010; Yadav et al. 2012; Liu et al. 2009).

In this paper, two-dimensional DFA and MFDFA are introduced into the analysis of a UIS pattern. The main aims of this study are to: (1) reveal the UIS spatial dependence and its temporal changes by spatial autocorrelation analysis; and (2) explore the long-range dependence in the UIS spatial pattern using two-dimensional DFA and MFDFA. The study area and data used in this paper are first described, and then the methodology is presented for analysing the UIS spatial pattern. Finally, this paper discusses results, and how to apply Moran's I and two-dimensional DFA and MFDFA to better understand the evolution of the UIS pattern.

Study area and data

Study area

The downtown area of Shanghai, China, was selected as the study area, focusing within the outer ring road of the city (Fig. 1). Shanghai is the largest economic centre of China, with a registered population of 23.03 million in 2010 and a total area of 6340.5 km^2. Since the economic reform in 1978, Shanghai has experienced an accelerated urbanisation, with an urbanisation rate (the ratio of urban population to total population) increasing from 59 % in 1978 to 86 % in 2007 (Yue et al. 2012). Accordingly, the urban land cover has undergone significant changes, and the natural land cover has been changed into anthropogenic impervious surface, especially within the study area. Urban planning has matured as the city develops in Metropolitan Shanghai since the early 1990s, but several decision-making factors have encouraged Shanghai to develop more rapidly than other cities in China (Yue et al. 2007). Detecting spatial dependence of UIS pattern might contribute to urban development in the future.

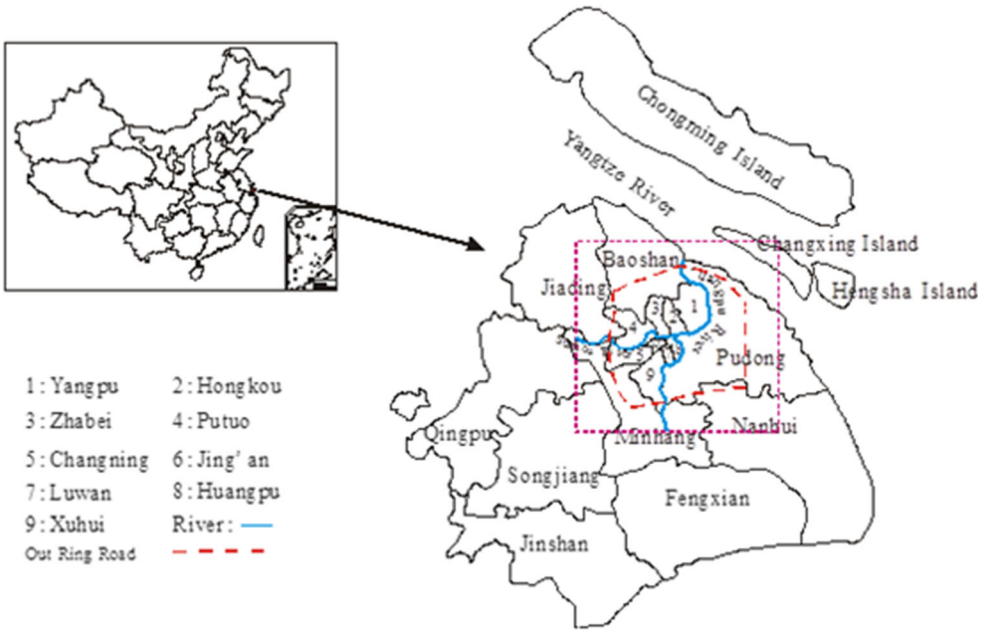

Fig. 1 Map of the study area

Data

Four cloud-free Landsat Thematic Mapper (TM) and Enhanced Thematic Mapper Plus (ETM+) images, acquired in 1997, 2002, 2007, and 2010, served as the primary data sources for mapping UIS in the study area. All images were preprocessed as follows. They were first registered to 1:10,000 topographic maps of Shanghai. It was assumed that the atmospheric conditions within the study area were homogeneous, so no atmospheric corrections were performed. The images were then further rectified to a Shanghai coordinate system (a modified Transverse Mercator coordinate system). The resultant root mean square (RMS) values were found to be less than 0.5 pixels.

Methodology

UIS estimation

UIS was estimated by linear spectral mixture analysis (LSMA). In urban studies, LSMA has shown the potential for estimating UIS. As a physically based image processing method, LSMA assumes that the spectrum measured by a sensor is a linear combination of the spectra of all components (endmembers) within the pixel. According to Small (2001), urban reflectance can be described with a three-component linear mixture model spanned by high albedo, low albedo, and vegetation endmembers. A typical LSMA model can be expressed as follows (Small 2001):

$$R_i = \sum_{k=1}^{n} f_k R_{ik} + \mathrm{ER}_i \quad (1)$$

where i is the number of spectral bands, k is the number of endmembers, R_i is the spectral reflectance of band i containing all endmembers, f_k is the proportion of endmember k within the pixel, R_{ik} is the known spectral reflectance of endmember k within the pixel on band i and ER_i is the error for band i.

The research team (Yue et al. 2006, 2007, 2009) has performed a large number of experiments in the study area taking ground measurements by wavelength dispersive spectrometer. Three endmembers including vegetation, high-albedo surfaces, and low-albedo surfaces can describe the urban reflectance of the study area well after masking the water body. Thus, in this study, $k = 3$, and includes vegetation (trees and grass), high-albedo surfaces (metal structures, new concrete surfaces, sand and some compound materials), and low-albedo surfaces (old concrete surfaces, cyan tiles and asphalt). A sum of the high-albedo and low-albedo fractions was applied to determine UIS.

A constrained least-squares solution was used, assuming that the following two conditions are simultaneously satisfied, as follows (Small 2001):

$$\sum_{k=1}^{n} f_k = 1 \text{ and } 0 \le f_k \le 1 \quad (2)$$

RMS error images were used to determine the overall error of all the end member abundance values for each pixel. A lower RMS error of the abundance images is desired, where:

$$\mathrm{RMS} = \sqrt{\sum_{i=1}^{m} \mathrm{ER}_i^2 / m} \quad (3)$$

The RMS image appears as noise and determines the overall error of all of the end member abundance values for each pixel. The areas with a high RMS error indicate low accuracy of spectral unmixing.

The accuracy assessment was conducted by two methods. The RMS for every image pixel was first calculated. The areas with high RMS error indicate low accuracy of spectral unmixing. Figure 2 illustrated the RMS frequency distribution and spatial image in 1997. As showed in Fig. 2, the RMS error values less than 0.015 account for the majority of the pixels. The spatial distribution image of RMS error indicated that the UIS fraction tended to be overestimated around the outer ring road. By linked to the corresponding aerial image, it is found that these regions were all high-albedo features, such as Shanghai Stadium, Hongkou Stadium, etc. The IS fraction overestimated may be due to the building materials of these high-albedo features. For the other study years, the mean of RMS error is all less than 0.02, which suggests a generally good fit. Secondly, a random sampling method was applied to assess accuracy of UIS estimation. For 1997 and 2002, the corresponding aerial image was used to obtain UIS fraction. The UIS fraction of the samples was got from high resolution image for 2008 and 2010. A sampling unit of 150 × 150 m was used and 100 samples in the image were chosen. Figure 3 showed the difference between estimation values and actual values of UIS fraction in 1997. The difference between estimation values and actual values is within ± 0.15. For the other years, the difference is within ± 0.2. Overall, the results of IS fraction estimation are reliable.

Moran's index (Moran's *I*)

Moran's I was used to test the presence of spatial dependence of UIS pattern at the pixel scale (i.e., 30 m). Moran's I is a measure of spatial autocorrelation-how related the values of a variable are based on the locations where they were measured, which can be defined as follows.

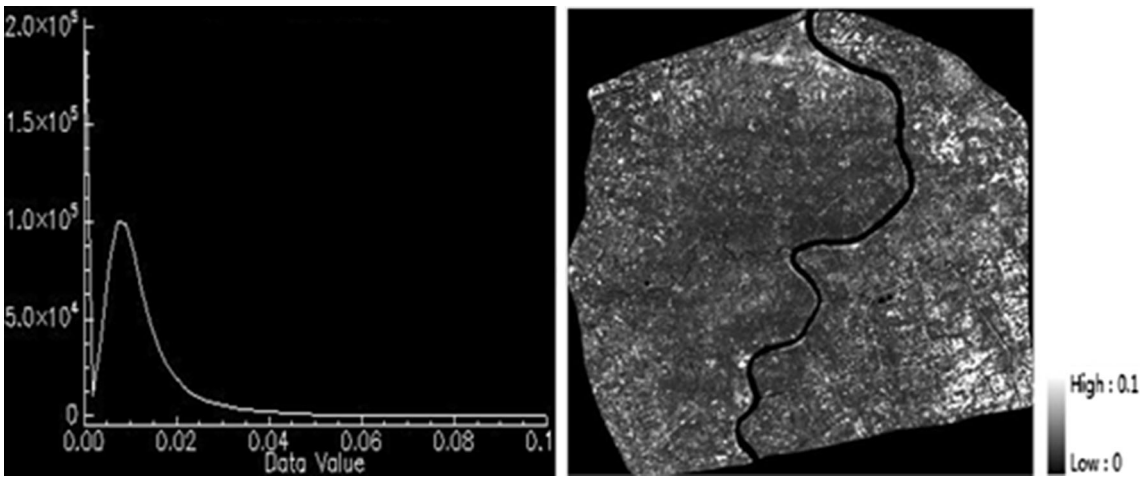

Fig. 2 The RMS frequency distribution and spatial image in 1997

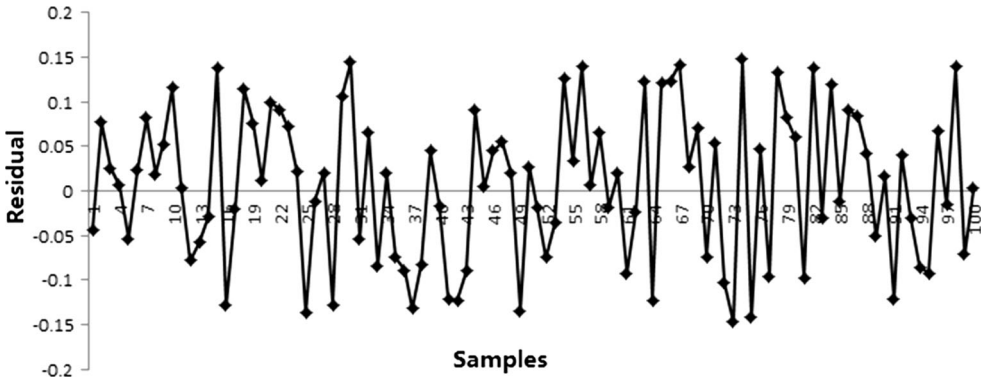

Fig. 3 The accuracy assessment of the impervious surface estimation in 1997

$$I = \frac{n\sum_{i=1}^{n}\sum_{j=1}^{n}\omega_{i,j}(x_i-\bar{x})(x_j-\bar{x})}{\sum_{i=1}^{n}\sum_{j=1}^{n}\omega_{i,j}\sum_{i=1}^{n}(x_i-\bar{x})^2} \quad (4)$$

where n is the number of spatial units indexed by i and j, x_i and x_j are the interested variables of neighbour pixels, $\bar{x}$ is the mean of X, and $\omega_{i,j}$ is an element of a matrix of spatial weights.

For statistical hypothesis testing, Moran's I values can be transformed to Z-scores in which values greater than 1.96 or smaller than -1.96 indicate spatial autocorrelation that is significant at 5 % level. The value of Moran's I range from -1 (indicating perfect dispersion) to 1 (perfect correlation), with negative (positive) values indicating negative (positive) spatial autocorrelation and a zero value indicating a random spatial pattern.

Two-dimension DFA and MFDFA

Two-dimensional DFA and MFDFA were employed to explore the long-range dependence of UIS spatial pattern. The two-dimensional DFA and MFDFA can be referred to the original source (Gu and Zhou 2006) for a detailed description of the method.

Given a two-dimensional array $X(i, j)$, $i = 1, 2,\ldots M$ and $j = 1, 2,\ldots N$, the array X is partitioned into $M_s \times N_s$ ($M_s = [M/s]$, $N_s = [N/s]$) disjoint square segments $X_{v,\,w}$, the cumulative sum $u_{v,\,w}(i, j)$ is calculated as:

$$u_{v,w}(i,j) = \sum_{k1=1}^{i}\sum_{k2=1}^{j} X_{v,w}(k1,k2) \quad (5)$$

where $1 \le i, j \le s$.

The trend of the cumulative sum, $\tilde{u}_{v,w}$, can be determined by fitting it with least square method. The residual matrix can be obtained:

$$\in_{v,\mathrm{w}}(i,j) = u_{v,w}(i,j) - \tilde{u}_{v,w}(i,j) \quad (6)$$

the detrended fluctuation function of the segment $X_{v,w}$ is defined as:

$$F^2 v,w,s = \frac{1}{s^2}\sum_{i=1}^{s}\sum_{j=1}^{s}\in_{v,w}(i,j)^2 \quad (7)$$

the overall detrended fluctuation is calculated by averaging over all the segments:

$$F^2(s) = \frac{1}{M_s N_s}\sum_{v=1}^{M_s}\sum_{w=1}^{N_s}F^2(v,w,s) \quad (8)$$

by varying the values of s, the scaling relation between $F(s)$ and s can be obtained:

$$F(s) \sim s^{2\alpha} \tag{9}$$

where α is scaling exponent. If $\alpha = 0.5$, long-range correlation is absent, and the array is random. In contrast, if $0.5 < \alpha < 1$, the positive power-law long-range correlation is presented, and $\alpha = 1$ correspond to $1/f$ noise. Values of $\alpha > 1$ indicate the presence of positive long-range correlation, but not the form of power-law correlation. The values of $0 < \alpha < 0.5$ indicate the presence of negative power-law long-range correlation.

Two-dimensional MFDFA is an extension of the DFA method. The method applied to experimental data of the present study can be summarised as follows (Yadav et al. 2012): the overall detrended fluctuation is calculated by averaging over all the segments,

$$F_q(s) = \left\{ \frac{1}{M_s N_s} \sum_{v=1}^{M_s} \sum_{w=1}^{N_s} [F(v,w,s)]^q \right\}^{1/q} \tag{10}$$

where q can take any real value except for $q = 0$.

When $q = 0$,

$$F_0(s) = \exp\left\{ \frac{1}{M_s N_s} \sum_{v=1}^{M_s} \sum_{w=1}^{N_s} \ln[F(v,w,s)] \right\} \tag{11}$$

Varying the value of s, the scaling relation between the detrended fluctuation function $F(s)$ and the scale s can be obtained:

$$F_q(s) \sim s^{h(q)} \tag{12}$$

If the scaling exponent $h(q)$ is a nonlinear function of q, the mass exponent $\tau(q)$ can be obtained:

$$\tau(q) = qh(q) - D_f \tag{13}$$

where D_f is the fractal dimension of the geometric support of the multifractal measure.

Finally, the singularity strength function $a(q)$ and the singularity spectrum $f(a)$ may be determined using the Legendre's transformation (Halsey et al. 1986).

Results and discussion

Visual interpretation of UIS pattern

Figures 4 provides an informative visual depiction of the spatial UIS patterns within the study area. Higher UIS values are distributed within the urban centre in 1997, especially across the old city in Puxing, the Wusong industrial zone, and the Huangpu River coast, with clear high–high aggregations. Conversely, the UIS fraction of parks, and green land is lower. The low–low aggregations

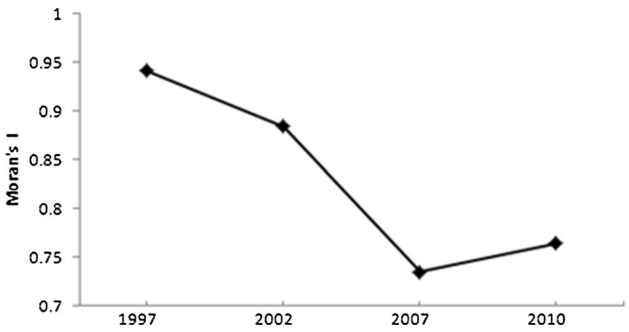

Fig. 4 Spatial pattern of UIS

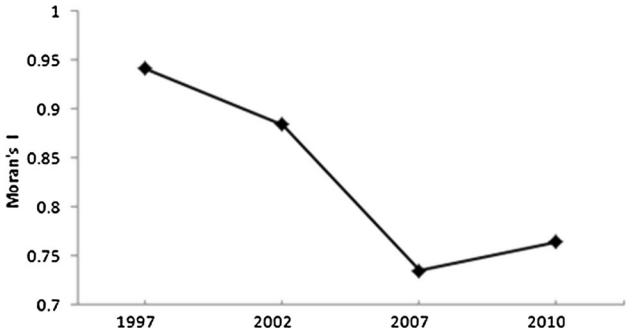

Fig. 5 Moran's I of UIS pattern

are obvious. In 2002, the high UIS values extend outwards from the 1997 spatial pattern, expanding to the outer ring road in Puxi. The UIS peaks are usually in areas where built-up areas, industries, and manufacturing factories are located. The high–high aggregations are clear. The changing trends of UIS are closely related to the urban sprawl of Shanghai.

The high UIS values, which tend to occur in clusters, had expanded to the outer ring road by 2007. By 2010, high UIS values dominate the study area, with 77.34 % of the pixels across the study area possessing UIS values greater than 80 %. The high–high aggregations become more obvious across the study period.

The analysis above reveals how UIS spatial patterns vary based on a visual interpretation. Overall, UIS increases and its spatial patterns change into a more contiguous pattern from 1997 to 2010, which is indicative of urban filling and expansion in downtown Shanghai.

Spatial dependence of the UIS pattern using Moran's *I*

To accurately reveal the spatial dependence of UIS pattern, Moran's I was calculated at the pixel scale (i.e., 30 m). As illustrated in Fig. 5, Moran's I is positive for the 4 years of the study, indicating the non-randomness in the UIS pattern. That is to say, that UIS patterns presented positive spatial dependence during the study period. Furthermore,

the index decreased from 1997 to 2007, and slightly increased from 2007 to 2010, suggesting that the spatial dependence highlighted a shift from aggregation to dispersion and back to aggregation during the study period.

Overall, the spatial dependence of the UIS pattern decreases during the study period, as indicated by the temporal change in Moran's *I*. Urbanisation is the main reason for this change. As mentioned in Sect. 4.1, the high UIS values were primarily concentrated in the old city, the Wusong industrial site, and industrial sites along the Huangpu River, whereas low values were mainly concentrated near the outer ring in 1997. These high values were usually near the high-fraction values and vice versa, with clear high–high and low–low aggregations.

However, this phenomenon was less obvious after rapid urbanisation. Since the 1990s, the city land paid use system has been implemented, leading to land use changes in the outer suburbs. With the strategy of Pudong development put forward by the Shanghai government, the focus of urban development in Shanghai shifted from Puxi to the Pudong region. These development zones, which include the Waigaoqiao Free Trade Zone and Jingqiao Export Processing District, were far from the original core urban area, creating spatial shifts in UIS. Additionally, the Shanghai government changed the urban development strategy from a production city to a habitability city, and Shanghai began the process of old city renewal and reconstruction. High UIS values spread rapidly, decreasing the global spatial dependence in the UIS pattern. Shanghai also made a new urban master plan in 2000 to promote balanced development between the cities in the Yangtze River Delta region. Since that time, the urbanisation of Shanghai entered a new stage, where large-scale residential buildings, satellite cities, industrial parks, and various kinds of functional zones have been built in the study area, creating a complex spatial UIS pattern.

Moran's *I* revealed the non-randomness of the UIS pattern from a single scale (i.e., 30 × 30 m), but cannot detect the spatial dependence from different spatial scales. Furthermore, it only revealed the spatial dependence of the neighbouring pixels. In the following section, fractal geometry will be used to detect the long-range dependence in the UIS spatial pattern.

Long-range dependence in the UIS spatial pattern

Double-logarithmic plots of the detrended fluctuations F versus size s, $ln\ (F(s)) \sim ln(s)$, were obtained to reveal the long-range dependence in the UIS spatial pattern. As illustrated in Fig. 6, the entire range of the function is linearly fitted, suggesting the existence of fractal properties of UIS pattern. It is interesting to note that the DFA scaling exponent a, which is the slope for each linear fit, exhibits

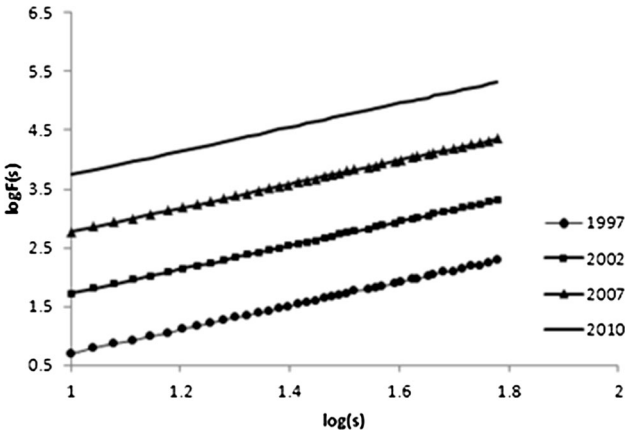

Fig. 6 Double-logarithmic plots of the detrended fluctuations F versus size s. The plots for 2002, 2007, and 2010 are shifted upward by 1, 2, and 3 for clarity

an approximate $1/f$ behaviour, as $a = 1 \pm 0.02$. This suggests that the UIS spatial pattern presents a strong long-range dependence, displaying a type of self-organised state.

The long-range correlations imply that the autocorrelation function decays as a power-law rather than exponentially. The strong long-range dependence identified signifies that the fluctuations in the UIS pattern, from small spatial intervals to larger ones, are positively correlated in a power-law fashion. This long-range dependence refers to the "long memory" or internal correlation within the spatial UIS pattern. For example, an increase in UIS fraction is followed by an increase in UIS values of a different spatial scale. This finding suggests that the correlations between the fluctuations in UIS fraction do not obey the classical Markov-type stochastic behaviour (exponential decrease with space), but rather decay in a slower fashion.

It is investigated that whether the strong long-range dependence found in the UIS pattern stems from the values of the UIS fraction themselves or from their spatial distribution. With this aim in mind, the two-dimensional array of UIS fractions was randomly shuffled. If the shuffled array follows the random (white) noise, then the long-range correlation found above does not originate from the data, but rather from their spatial distribution. The application of the two-dimensional DFA to the shuffled array gives $a = 0.5 \pm 0.02$, which reveals that the shuffled UIS fraction array is uncorrelated. Therefore, the power-law relationship eventually stems from long-range spatial correlations.

It should be emphasised that a can be seen as reflecting the degree of uniformity in UIS spatial distribution. As a increases, the long-range correlation strengthens, the fluctuation between UIS fraction slows, and the UIS fraction spatial pattern becomes more homogeneous. In contrast, decreasing a speeds the fluctuations and strengthens

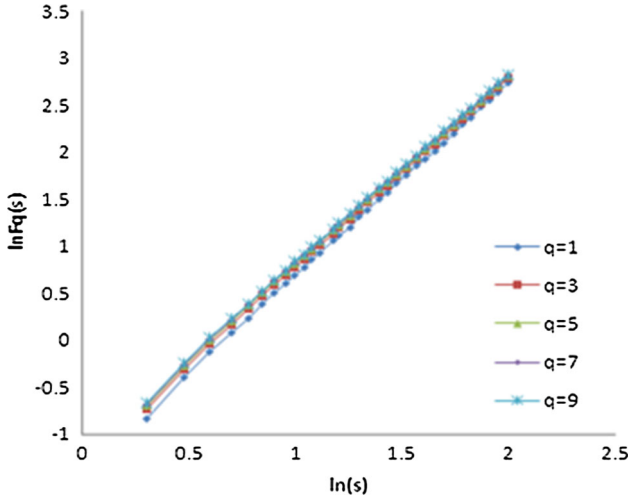

Fig. 7 Log–log plots of detrended fluctuation function F_q (s) versus scale s for five different values of q in 1997. The lines are the best power-law fits to the data

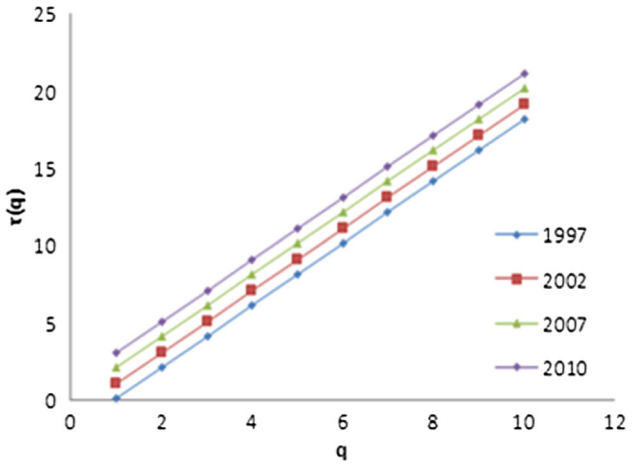

Fig. 8 The mass exponent function τ (q). The plots for 2002, 2007, and 2010 are shifted upward by 1, 2, and 3 for clarity

the spatial heterogeneity of UIS fraction. Thus, the DFA scaling exponent is a very useful measure for capturing the spatial variation in UIS.

Two-dimensional DFA only used a single scaling exponent to identify the long-range dependence in the UIS spatial pattern. In order to detect the long-range correlation from multiple levels, two-dimensional MFDFA can be used to reveal the correlation using a series of scaling exponents. Next, this paper used two-dimensional MFDFA to investigate the long-range dependence in UIS pattern.

Two-dimensional MFDFA was first performed to check if the UIS spatial pattern possesses a multifractal nature. The results indicate that, for negative values of q, the detrended fluctuation function $F_q(s)$ is linear in double-logarithmic coordinates. The 1997 spatial pattern is taken as an example to illustrate the power-law scaling between $F_q(s)$ and the scale s. Figure 7 shows $F_q(s)$ as a function of s for five different values of q in double-logarithmic coordinates. The data points for every q-value fall on a straight line, indicating a perfect power-law scaling between $F_q(s)$ and s. For $q > 0$, $F_q(s)$ in 2002, 2007, and 2010 also exhibits power-law behaviour. The slope of each straight line is the scaling exponent$\tau(q)$, which can be determined by linear regression of $ln(F_q(s))$ against $ln(s)$ for different q-values. Figure 8 illustrates $\tau(q)$ as a function of q for $q > 0$. The strong linear relationship between $\tau(q)$ and q confirms that the spatial patterns of the UIS does not possess a multifractal nature, and only a scaling exponent is required to disclose the long-range correlation in UIS spatial patterns.

It is worth noting that, for negative values of q, F_q(-s) shows nonlinearity in double-logarithmic coordinates. This is mainly related to the frequency distribution of UIS fraction. The low fraction values account for small numbers. Taking the UIS pattern in 2002 and 2010 as an example, the present study obtained the frequency maps of fraction distribution (Fig. 9). As shown in Fig. 9, it is clear that a fraction value of less than 0.8 is small in the 2 years examined, especially in 2010. The mean UIS fraction in 2002 and 2010 was 0.82 and 0.85, respectively. Similar frequency distribution maps were found in 1997 and 2007. In the calculation of MFDFA, negative values of q are

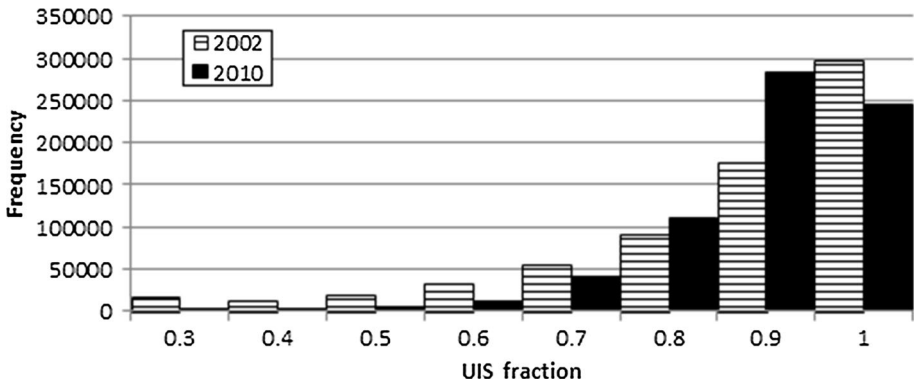

Fig. 9 Frequency map of UIS fraction in 2002 and 2010

associated with the fluctuation of low fraction values. When $q < 0$, $F_q(s)$ changes little with respect to s due to the small proportion of the low fraction pixel in the study area. Thus, $ln(F(s)) \sim ln(s)$ exhibits a nonlinear relationship for negative q-values.

The application of two-dimensional DFA and MFDFA to UIS patterns presented in this paper should be viewed as a complementary tool to existing techniques (e.g., Fourier analysis, wavelets, and structure function), aimed at providing a systematic characterisation of UIS patterns. In particular, box-counting methods are useful in the characterisation of UIS patterns (Nie et al. 2014). The DFA used in this paper can provide additional information about the structure of UIS patterns, such as the $1/f$ behaviour associated with the UIS pattern. A detailed theoretical investigation will be conducted in the future to determine the origin of the long-range dependence in the UIS spatial pattern.

Conclusions

This paper analyzes satellite data from downtown Shanghai, China, to introduce two-dimensional DFA and MFDFA as a new and complementary tool that provides additional information on the long-range dependence of UIS spatial patterns. The UIS spatial pattern exhibits a positive spatial dependence, as revealed by Moran's I, whose temporal change demonstrates the spatial dependence from aggregation to dispersion and back to aggregation during the 1997–2010 period. Urbanisation is the main reason for this change. Moreover, two-dimensional DFA shows that the UIS spatial pattern exhibits a strong long-range power-law dependence during the study period. The DFA scaling exponent highlights an approximate $1/f$ behaviour, and can be seen as a measure of the uniformity of the UIS spatial distribution. The larger the scaling exponent, the slower the fluctuation between the UIS fraction, and the more homogenised the UIS spatial pattern. Additionally, two-dimensional MFDFA shows that the UIS spatial patterns do not possess a multifractal nature, and only a single scaling exponent is required to disclose the long-range dependence in the UIS spatial pattern.

Acknowledgments This work was supported by the National Natural Science Foundation of China (Grant no. 41102224; 41130525).

References

Barrera E, Gonzalez F, Rodriguez E, Alvarez-Ramirez J (2010) Correlation of optical properties with the fractal microstructure of black molybdenum coatings. Appl Surf Sci 256(6):1756–1763

Bauer ME, Heinert NJ, Doyle JK, Yuan F (2004) Impervious surface mapping and change monitoring using Landsat remote sensing. ASPRS annual conference proceedings, May 23–28, 2004, Denver, Colorado

Clapham WB Jr (2003) Continuum-based classification of remotely sensed imagery to describe urban sprawl on a watershed scale. Remote Sens Environ 86:322–340

Dougherty M, Dymond RL, Goetz SJ, Jantz CA, Goulet N (2004) Evaluation of impervious surface estimates in a rapidly urbanizing watershed. Photogramm Eng Remote Sens 70(11):1275–1284

Gu GF, Zhou WX (2006) Detrended fluctuation analysis for fractals and multifractals in higher dimensions. Phys Rev E 74(6):061104

Halsey TC, Jensen MH, Kadanoff LP, Procaccia I, Shraiman BI (1986) Fractal measures and their singularities: the characterization of strange sets. Phys Rev A 33(2):1141–1151

Liu C, Jiang XL, Liu T, Zhao L, Zhou WX, Yuan WK (2009) Multifractal analysis of the fracture surfaces of foamed polypropylene/polyethylene blends. Appl Surf Sci 255(7):4239–4245

Liu ZH, Wang YL, Peng J, Xie MM, Li Y (2011) Using ISA to analyze the spatial pattern of urban land cover change: a case study in Shenzhen (in Chinese). Acta Geogr Sinica 66(7):961–971

Liu ZH, Wang YL, Peng J (2012) Quantifying spatiotemporal patterns dynamics of impervious surface in Shenzhen (in Chinese). Geogr Res 31(8):1535–1545

Moktadir Z, Kraft M, Wensink H (2008) Multifractal properties of Pyrex and silicon surfaces blasted with sharp particles. Physica A Stat Mech Appl 387(8):2083–2090

Nie Q, Xu JH, Liu ZH (2014) Fractal and multifractal characteristic of spatial pattern of urban impervious surfaces. Earth Sci Inform. doi:10.1007/s12145-014-0159-1

Raoufi D, Fallah HR, Kiasatpour A, Rozatian ASH (2008) Multifractal analysis of ITO thin films prepared by electron beam deposition method. Appl Surf Sci 254(7):2168–2173

Rashed T (2008) Remote sensing of within-class change in urban neighborhood structures. Computers Environ Urban Syst 32(5):343–354

Relly J, Maggio P, Karp S (2004) A model to predict impervious surface for regional and municipal land use planning purposes. Environ Impact Assess Rev 24(3):363–382

Small C (2001) Estimation of urban vegetation abundance by spectral mixture analysis. Int J Remote Sens 22:1305–1334

Xian G, Crane M (2006) An analysis of urban thermal characteristics and associated land cover in Tampa Bay and Las Vegas using Landsat satellite data. Remote Sens Environ 104(2):147–156

Xie MM, Wang YL, Li GC (2009) Spatial variation of impervious surface area and vegetation cover based on subpixel model in Shenzhen (in Chinese). Resour Sci 31(2):257–264

Yadav RP, Dwivedi S, Mittal AK, Kumar M, Pandey AC (2012) Fractal and multifractal analysis of LiF thin film surface. Appl Surf Sci 261(8):547–553

Yue W (2009) Improvement of urban impervious surface estimation in Shanghai using Landsat7 ETM+ data. Chin Geogr Sci 19:283–290

Yue WZ, Xu JH, Wu JW, Xu LH (2006) remote sensing research on the spatial pattern of reconstruction of old city based on Linear spectral analysis (in Chinese). Kexue Tongbao 51(8):966–974

Yue W, Xu J, Tan W, Xu L (2007) The relationship between land surface temperature and NDVI with remote sensing: application to Shanghai Landsat 7 ETM+ data. Int J Remote Sens 28:3205–3226

Yue W, Liu Y, Fan P, Ye X, Wu C (2012) Assessing spatial pattern of urban thermal environment in Shanghai, China. Stoch Environ Res Risk Assess 26:899–911